Eur. Phys. J. A **8**, 493–499 (2000)

THE EUROPEAN PHYSICAL JOURNAL A

Analysis of the spectator-angular distribution in the light-nuclei reactions

A. Dirner[1], V.V. Glagolev[2], J. Hlaváčová[3], N.B. Ladygina[2], G. Martinská[1,a], and J. Urbán[1]

[1] University of P.J.Šafárik, Jesenná 5, SK-04154 Košice, Slovak Republic
[2] Joint Institute for Nuclear Research, 141980 Dubna, Russia
[3] Technical University, Park Komenského 2, SK-04200, Košice, Slovak Republic

Received: 11 February 2000 / Revised version: 20 June 2000
Communicated by B. Povh

Abstract. Angular distributions of spectator particles in dp and ^{4}Hep reactions in the region of a few GeV have been studied. Significant asymmetries of the spectator particle distributions have been observed for reactions where π-mesons are produced in the final state. Results of calculations in the framework of a spectator model taking into account the nuclear wave function, flux factor and the energy dependence of the NN elementary cross-sections, have been compared to experimental data. A good agreement has been observed for the fragments momenta, where the one-pole mechanism dominates.

PACS. 25.10.+s Nuclear reactions involving few-nucleon systems – 25.60.Gc Breakup and momentum distributions

1 Introduction

The study of angular distributions from spectators in interactions of light nuclei with protons is of basic interest from the point of view of various reaction mechanisms validity and also for the interpretation of the results obtained by different experimental methods.

The analysis of light-nuclei fragmentation reactions has shown that the main process here is the one-pole mechanism and simple models within the impulse approximation do reproduce the spectator momentum distribution at small momenta, up to 100–300 MeV/c, depending on the nuclei. The momentum distribution of spectators is then simply obtained from the wave function in the momentum representation. This approximation assumes an isotropic angular distribution of the nucleons, reflecting the Fermi motion inside the nucleus. Assuming further the validity of a factorization of the amplitudes in the vertices of the pole diagram the isotropy is supposed to be unchanged during the interaction (for the quasi-NN reaction). This approximation is applied to both quasielastic and inelastic processes.

As it has been demonstrated in our previous papers dealing with reaction where no real π-meson is produced [1], the nuclear fragments are "passive" spectators as they only slightly effect the interaction. In the present work the data on dp and ^{4}Hep reactions are presented where at least one pion is observed in the final state. A significant anisotropy has been measured in the angular distributions of the nuclear fragments in such reactions. The aim of the present paper is to show that the observed substantial deviation from the isotropic angular distribution of the nuclear fragments does not contradict the spectator model, at least in the region of the fragment momenta below 200 MeV/c for dp and below 350 MeV/c for ^{4}Hep reactions, where the spectator model predictions are in good agreement with the experimental data [1].

In earlier investigations similar to the one presented here, the inelastic reactions with pion production in the proton-deuteron scattering at 1.825 GeV/c and 2.11 GeV/c have been studied using a deuterium bubble chamber in [2]. The impulse approximation was valid up to a spectator momentum of 150 MeV/c, but the low momentum part, *i.e.* momenta below 80 MeV/c, was inaccessible for those experiments.

In the fragmentation studies a new way of data representation is suggested in terms of the relative four-velocity squared and the self-similarity behaviour of these processes is demonstrated [3].

2 Experiment

The interactions of accelerated d and ^{4}He nuclei have been investigated by analysing the pictures taken at the JINR LHE 1m hydrogen bubble chamber (HBC), which is simultaneously both a pure proton target and a full solid angle detector. The momentum of the d was 3.34 GeV/c and the momenta of ^{4}He were 8.6 and 13.6 GeV/c. The use of nuclear beams impinging on a fixed proton target makes all the fragments of the incoming nuclei fast in the laboratory

[a] e-mail: martinov@kosice.upjs.sk

Table 1. Cross-sections of the reactions with pion production.

No	Reaction	Momentum per nucleon (GeV/c)	σ (mb)	Corresponding quasi-NN subprocess
1	$dp \to ppp\pi^-$	1.67	1.88 ± 0.03	$np \to pp\pi^-$
2	$dp \to ppn\pi^+\pi^-$	1.67	0.35 ± 0.01	$np \to pn\pi^+\pi^-$ $pp \to pp\pi^+\pi^-$
3	$dp \to dn\pi^+$	1.67	1.70 ± 0.02	$pp \to d\pi^+$
4	$^4Hep \to ^3Hpn\pi^+$	2.15	11.50 ± 0.21	$pp \to pn\pi^+$
		3.4	6.90 ± 0.18	
5	$^4Hep \to ^3Hepn\pi^+\pi^-$	2.15	1.84 ± 0.09	$pn \to pn\pi^+\pi^-$
		3.4	3.40 ± 0.12	

frame and, thus, they can be detected, well measured and identified practically without losses. These conditions and the full solid angle geometry allow to study the reaction channels containing not more than one neutral particle in an exclusive approach and to make conclusions about the accompanying effects. The geometrical reconstruction of tracks measured from 3 (4) stereo-projections and the subsequent kinematical analysis have been carried out using the CERN program system based on HYDRA package [4].

In the present work channels with not more than one neutral particle are discussed. All quantities in the following, if not stated explicitly otherwise, are to be understood with respect to the projectile nucleus rest frame (antilaboratory frame), in order to compare our results with other experimental results.

3 Results and discussion

The fragmentation process is schematically shown in fig. 1. As a passive spectator fragment A′ of the initial nucleus is supposed to have only small influence on the reaction mechanism as a whole, identified as the slowest baryon in the initial nucleus rest frame. It is reasonable under these conditions to expect a quasi-free NN interaction in the upper vertex (fig. 1). In the studied cases the exchanged particle in the upper vertex is an off-shell nucleon (see table 1) and A′ is certainly on-shell.

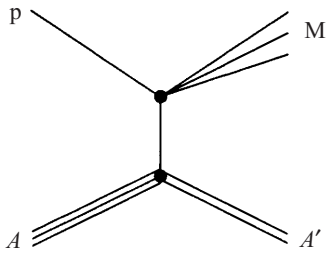

Fig. 1. Schematical representation of the fragmentation process.

Reactions with pion production have been studied, which offer the possibility to learn about different reaction mechanisms. In particular one may ask whether the spectator scenario is applicable to the inelastic fragmentation reactions. In table 1 the cross-sections of the investigated reactions with pion production together with their associated quasi nucleon-nucleon reactions (upper vertex in fig. 1) are listed. The analysis of the nuclear fragment production carried out for the reaction channels where no real π-meson is produced showed a typical spectator like behaviour: the momentum spectra could be acceptably described by known wave functions up to 100–250 MeV/c depending on the initial nuclei and the angular distributions were isotropic [1]. The nuclear fragments are of similar nature in the channels with pions, as it is illustrated by fig. 2, where their momentum distributions are shown together with the corresponding wave functions (Paris and Bassel-Wilkin) for the case of $dp \to p_s pp\pi^-$ and $^4Hep \to ^3He_s pn\pi^+\pi^-$ reactions. Subscript "s" denotes the slowest particle (except for pions) and is referred to as a spectator. It can be seen that the used wave functions reasonably describe the experimental data up to momentum values of 200 MeV/c for dp and 350 MeV/c for the ^{4}Hep reactions. The curves are normalized to the maximum of the experimental distributions.

One of the possible ways how to estimate the deformation of the spectator production angle distribution is to include the energy dependence of the quasi-NN cross-section $\sigma(s)$ and the flux factor. Assuming an unpolarized nucleus the Fermi momentum distribution should be isotropic and the measured spectator angular distribution can be written as

$$\frac{\mathrm{d}\sigma}{\mathrm{d}(\cos\Theta_\mathrm{s})} = \int_0^p p_\mathrm{s}^2 |\Phi(p_\mathrm{s})|^2 \sigma(s) F(p_\mathrm{s}, p_\mathrm{b}, \cos\Theta_\mathrm{s})\,\mathrm{d}p_\mathrm{s}, \quad (1)$$

where subscript s denotes the spectators production angle (Θ_s) and momentum (p_s), subscript b means the initial proton, s stands for the total quasi-NN c.m.s. energy (includes Fermi motion and off-shellness), $\Phi(p_\mathrm{s})$ is the initial nucleus wave function in momentum representation, $\sigma(s)$ is the energy-dependent cross-section of the reaction in

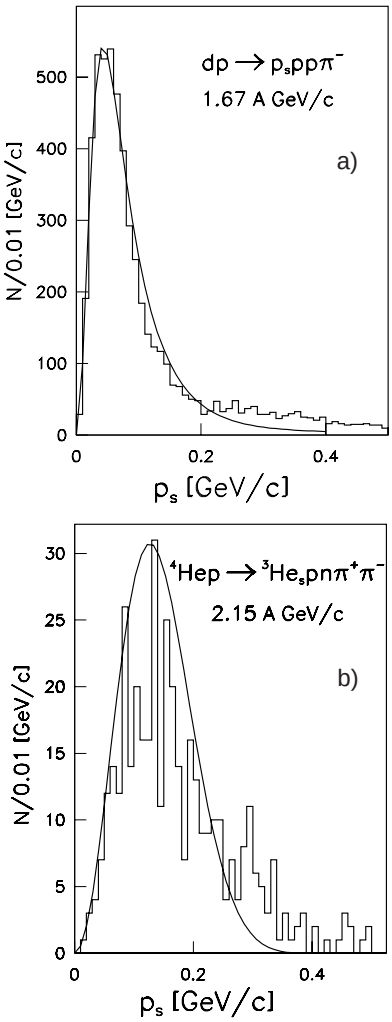

Fig. 2. Spectator momentum distributions (histograms) compared with wave functions (solid lines): Paris wave function for dp (a) and Bassel-Wilkin wave function for ^{4}Hep (b).

the upper vertex and

$$F(p_\mathrm{s}, p_\mathrm{b}, \cos\Theta_\mathrm{s}) = \frac{1}{m_\mathrm{R} m_\mathrm{b}} \times \Big[(E_\mathrm{b}E_\mathrm{R} + p_\mathrm{b}p_\mathrm{s}\cos\Theta_\mathrm{s})^2 - m_\mathrm{b}^2 m_\mathrm{R}^2\Big]^{1/2}$$

is the flux factor [5]. Within the used model it is expected that the spectator momentum is only slightly affected by the upper vertex and so the Fermi momentum of the exchanged nucleon R is equal to that of the spectator A′ with opposite orientation: $\mathbf{p}_\mathrm{R} = -\mathbf{p}_{\mathrm{A}'} = -\mathbf{p}_\mathrm{s}$.

To characterize the angular distributions, one can introduce the asymmetry $A = [N(\Theta < 90^\circ) - N(\Theta > 90^\circ)]/[N(\Theta < 90^\circ) + N(\Theta > 90^\circ)]$, where $N(\Theta < 90^\circ)$ and $N(\Theta > 90^\circ)$ are the numbers of events with spectators in the forward and backward hemispheres, respectively. Figure 3 shows the angular distributions of spectators together with the results of calculations using formula (1) for different reactions. In each case the curves are individually normalized for the absolute values to the experimental distributions.

The main mechanism of the reaction ^{4}Hep→^{3}He$_\mathrm{s}$pn is the one-pole mechanism with quasielastic pn → pn scattering while the ^{3}He is a spectator [1]. As the elastic pn → pn reaction is almost energy independent in our energy region there is no contribution of $\sigma(s)$ to formula (1) for this reaction and the asymmetry is as small as $A = 0.05 \pm 0.02$ (fig. 3c). The small inhomogenity in the latter may be due to the presence of other mechanisms, *e.g.*, final-state interaction [6,7].

Significant asymmetries of different sign in reactions with π-meson production (fig. 3a),b),d)) have been observed in the spectator angular distributions. The corresponding experimental and calculated asymmetries are presented in table 2, where only fragments with momenta $p_{\mathrm{A}'} < 200\,\mathrm{MeV/c}$ for dp and $p_{\mathrm{A}'} < 350\,\mathrm{MeV/c}$ for ^{4}Hep reactions have been analyzed. This effect is more demonstrative in the reactions: i) with two pions than in those where only a single pion is produced and ii) at lower beam energies. Such an asymmetry is not only of a pure kinematical origin.

In the case of reactions with pion production the dependence of cross-section on the reaction energy is very remarkable. As an example, in fig. 4 the energy dependence of the NN cross-section is displayed for reactions 3 and 2 (or 5). The reaction c.m.s. energies squared $s = 5.35$, respectively, 6.16 and $8.38\,\mathrm{GeV}^2$ corresponding to incoming proton momenta 1.67 (in dp reaction), respectively, 2.15 and 3.4 GeV/c (in ^{4}Hep reactions), and with the target nucleon at rest, are in the steeply changing parts of the corresponding NN cross-sections, *i.e.* in the decreasing and increasing ones for the reaction (3) and for the others, respectively. The Fermi motion of the target nucleon yields an important spreading in the reaction energy and also modifies the kinematics of the studied subprocesses in the upper vertex fig. 1. This is shown in fig. 5, where the reaction energy distributions of the quasi-NN subprocesses of the reactions dp → p$_\mathrm{s}$ppπ^- and ^{4}Hep→^{3}He$_\mathrm{s}$pn$\pi^+\pi^-$ are displayed. So, the smearing in the reaction energy and the energy dependence of the corresponding subprocesses cross-sections are reflected in the angular distributions. The closer the beam energy to the threshold of the corresponding NN process the effect of Fermi motion becomes more emphasized. It means that higher reaction energies due to Fermi motion in the upper vertex result in smaller (more forward) angles for the spectator.

It can be seen from table 2 that $\sigma(s)$ dependence plays the main role in the calculated description of the experimental asymmetries. The angular distributions for nuclear fragments and the corresponding values of asymmetries confirm the above-mentioned hypothesis. For reactions 1, 2, 4, 5 remarkable data enhancements occur at forward scattering angles (the asymmetry values are positive). The asymmetry values increase with the number of pions produced in the reaction because for the case of two pions our energy is closer to the reaction threshold. Higher incoming momenta, on the other hand, are farther from the

Table 2. Asymmetries of the spectator angular distributions.

Reaction	Momentum per nucleon (GeV/c)	Asymmetry		
		experimental	calculated (1)	calculated (*)
$dp \to p_s pp\pi^-$	1.67	0.193 ± 0.015	0.133	0.044
$dp \to p_s pn\pi^+\pi^-$	1.67	0.667 ± 0.057	0.223	0.044
$dp \to n_s pp\pi^+\pi^-$	1.67	0.617 ± 0.110	0.886	0.044
$dp \to dn_s\pi^+$	1.67	-0.200 ± 0.027	-0.216	0.044
$^4Hep \to {}^3H_s pn\pi^+$	2.15	0.166 ± 0.019	0.071	0.084
	3.4	0.090 ± 0.030	-0.028	0.080
$^4Hep \to {}^3He_s pn\pi^+\pi^-$	2.15	0.869 ± 0.128	0.445	0.084
	3.4	0.474 ± 0.073	0.154	0.080

(*) is ([1]) without $\sigma(s)$.

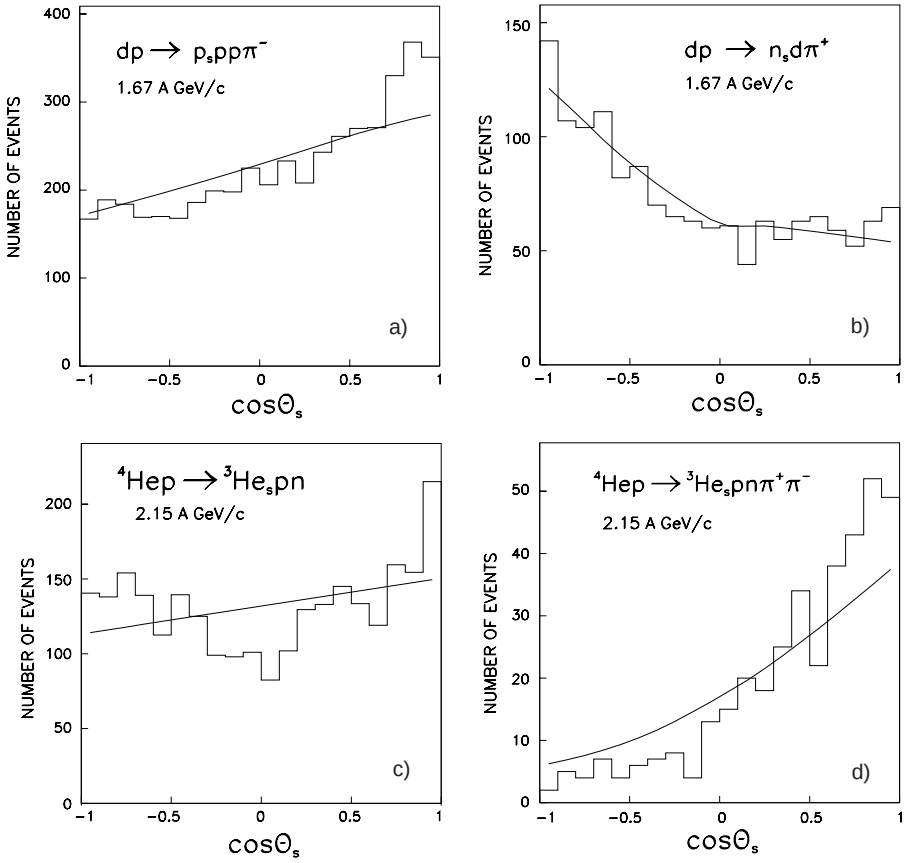

Fig. 3. Measured (histogram) and calculated angular distributions of spectators in dp (a,b) and ^{4}Hep (c,d) reactions.

reaction threshold, so it causes a decrease of asymmetry values.

For reaction 3 the value of asymmetry is negative, the enhancement is observed at backward angles. The reaction energy is in the falling part of the subprocess cross-section (see arrow in fig. 4a). On the other hand, quasi nucleon process $pp \to d\pi^+$ cross-section is peaked and is determined by the two proton relative momentum [9]. Now smaller relative momenta in the upper vertex fig. 1 need backward-produced spectators. So, in this way the reaction $dp \to n_s d\pi^+$ selects an event sample enriched with negative asymmetries.

Taking into account the cross-section energy dependence in expression (1) a qualitative agreement between the calculations and the data has been obtained also for the reactions with pion production within the spectator model, so the asymmetries observed do not contradict the spectator model.

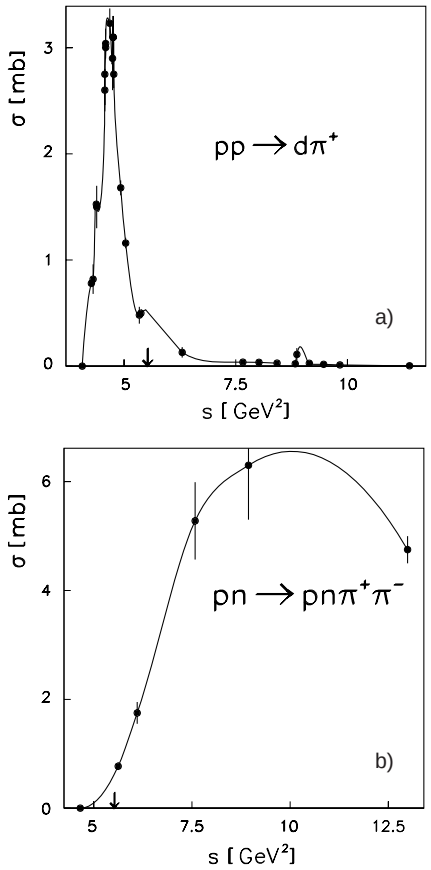

Fig. 4. NN cross-section σ *vs.* c.m.s. reaction energy s for $pp \to d\pi^+$ (a) and $pn \to pn\pi^+\pi^-$ (b) reactions; the data are taken from [8]. The arrow indicate our c.m.s. energy squared for dp interaction.

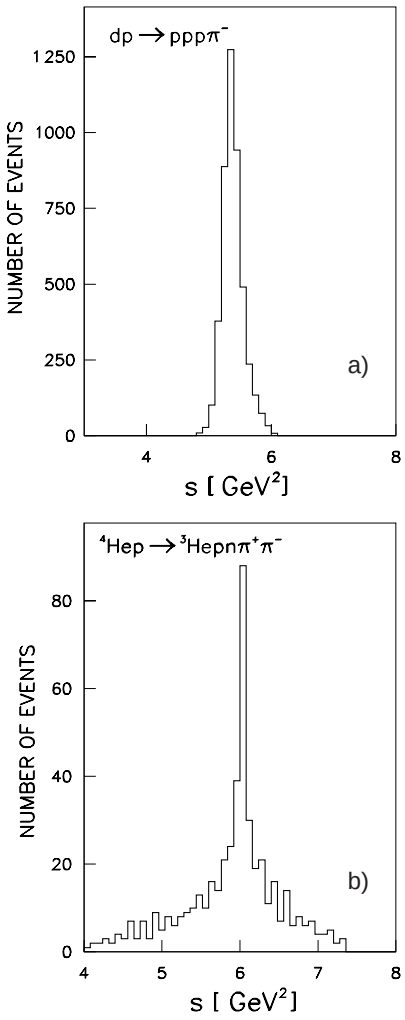

Fig. 5. The reaction c.m.s. energy distributions of the quasi NN subprocesses of the reaction $dp \to p_s pp\pi^-$ (a) and $^4\mathrm{Hep} \to {}^3\mathrm{He}_s pn\pi^+\pi^-$ (b). The bound nucleon is taken with momentum $\mathbf{p}_\mathrm{R} = -\mathbf{p}_\mathrm{s}$ and off-mass-shell.

The asymmetry of the spectator angular distribution is also reflected in an other variable, suitable for relativistic nuclear fragmentation reactions of the type

$$\mathrm{p} + \mathrm{A} \longrightarrow \mathrm{A}' + \mathrm{M}, \tag{2}$$

suggested in [3], differing from the Chew-Low plot mainly in the use of the relative four velocity squared

$$b_{\mathrm{AA}'} = -\left(\frac{P_\mathrm{A}}{M_\mathrm{A}} - \frac{P_{\mathrm{A}'}}{M_{\mathrm{A}'}}\right)^2, \tag{3}$$

[10] instead of the four-momentum transfer squared $|t|$. Here A and A′ are related to the parent nucleus and fragment, respectively and P stands for the corresponding four-momenta.

Another difference is the way of the normalization of the missing mass squared MM^2 to the studied fragment A′:

$$MM^2 = \left(P_\mathrm{p} + P_\mathrm{A} - P_{\mathrm{A}'}\right)^2 = \left[M_\mathrm{p}^2 + M_\mathrm{R}^2 + 2E_\mathrm{p}E_\mathrm{R}\right] + 2\mathbf{p}_{\mathrm{A}'} \cdot \mathbf{p}_\mathrm{p}, \tag{4}$$

where the expression in the squared brackets is the total c.m.s. energy squared (S') for the collision of the incoming particle (proton) with the rest (R) of the nucleus A, when the fragment A′ is excluded, corresponding to the upper vertex in fig. 1. From here follows the way how to use the quantity S', expressed in the recoiled on-mass-shell R rest frame as

$$S' = \left(P_\mathrm{p} + P_\mathrm{R}\right)^2 = M_\mathrm{p}^2 + M_\mathrm{R}^2 + 2E_pM_\mathrm{R}$$

for normalization purposes.

As an example for the fragmentation process, where no real π-meson is produced, fig. 6 displays the $^4\mathrm{Hep} \to {}^3\mathrm{Hpp}$ reaction data and the contour lines for two values of the proton momenta (2.15 and 3.4 A GeV/c). The "middle" line corresponds to A′ fragment production at 90° in the A nucleus rest frame, *i.e.* $\mathbf{p}_0 \cdot \mathbf{p}_{\mathrm{A}'} = 0$. The upper branch of the countour line corresponds to A′ fragment production at 0° while the lower one to its production at 180°. Experimental points, as it can be seen, are predominantly inside the corresponding contour lines. The points out-

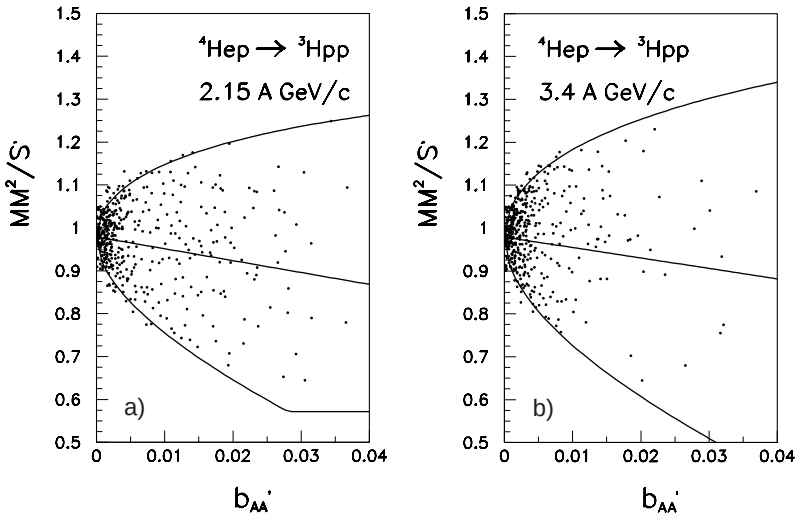

Fig. 6. The MM^2/S' *vs.* $b_{\mathrm{AA}'}$ plot for the ^{4}Hep→^{3}Hpp reaction at 2.15 A GeV/c (a) and at 3.4 A GeV/c (b).

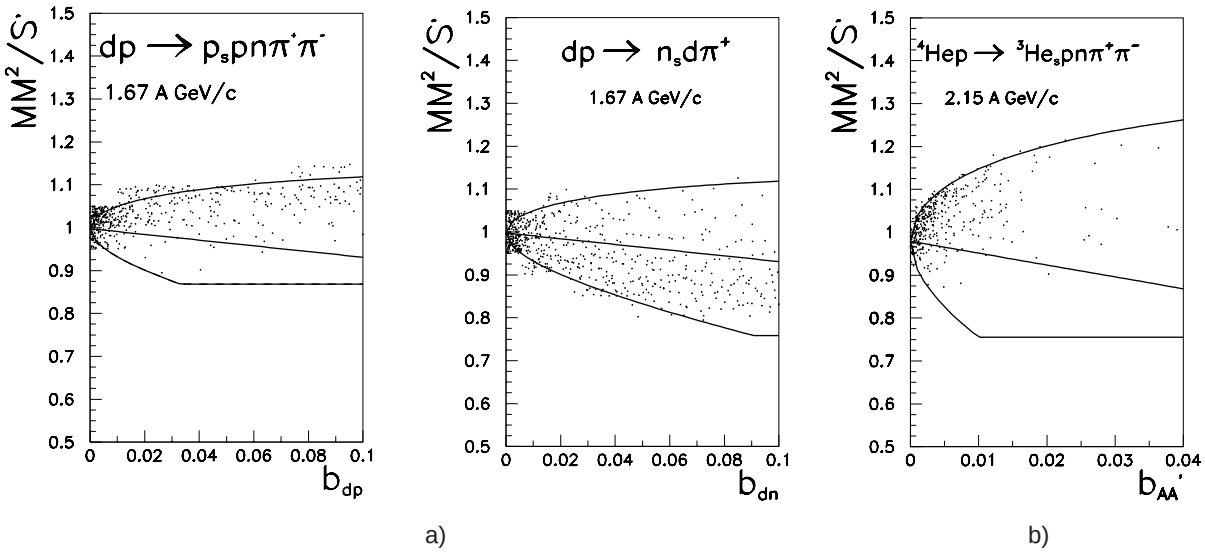

Fig. 7. The MM^2/S' *vs.* $b_{\mathrm{AA}'}$ plot for the dp (a) and ^{4}Hep (b) reactions.

side are connected with the errors of measurement. The events with a fragment triton are predominantly concentrated in the area of small $b_{\mathrm{AA}'}(< 0.04)$, as it has been predicted by [10]. Points are equally populated in the upper and lower parts around the "middle" line. Similar behaviour is observed in all investigated fragmentation processes, where no real π-mesons are produced [11]. Figure 7 displays experimental data with contour lines for pion containing reactions 2, 3 (a) and 5 (b) at the lower value of proton momentum. As it can be seen, the data are not equally populated inside the contour lines as it is in the cases of fragmentation processes without real π-meson production (fig. 6). Apart from the reaction 3 there is a clear tendency in the experimental data to concentrate above the middle line. In the case of reaction (3) the lower part is more densely populated than the upper one. These results reflect the observed asymmetries in the angular distributions.

4 Conclusion

Deuteron-proton and ^{4}He-proton reactions with pion production have been studied at different incoming momenta. A significant asymmetry in the spectator production angle distribution has been observed. Other manifestation of this effect is the remarkably unequal data population in the upper and lower parts of MM^2/S' *vs.* $b_{\mathrm{AA}'}$ plots. The influence of the Fermi motion on the kinematics of the studied processes is analyzed. The Fermi motion of the target nucleon yields an important spread in the c.m.s. energy and hence modifies the kinematics of the studied processes.

It has been shown that the energy dependence of the NN cross-section remarkably influences the angular asymmetry in the reactions with pion production. The asymmetry becomes more significant for s values close to the π threshold as well as for s belonging to the steeply changing region of the NN subprocess cross-section $\sigma(s)$. The

asymmetry strongly depends on the reaction energy and increases with the number of pions in the reaction since at our energies (close to the threshold) the nucleon-nucleon cross-sections are strongly energy dependent.

While in the fragmentation processes without real π-meson production, where the $\sigma(s)$ dependence is very weak, the spectator angular distributions are almost isotropic, the anisotropy in the reactions with pion production, due to the strong energy dependence of the NN cross-section, can also be reproduced in the framework of the spectator model.

This work was partly supported by the Grant Agency for Science at the Ministry of Education of the Slovak Republic (grant No. 2/5057/98).

References

1. V.V. Glagolev *et al.*, Phys. Rev. C **18**, 1382 (1978); P. Zielinski *et al.*, Yad. Fiz. (J. Nucl. Phys.) **43**, 791 (1986).
2. D.C. Brunt, M.J. Clayton, B.A. Westwood, Phys. Rev. **187**, 1856 (1969).
3. V.V. Glagolev, G. Martinská, J. Urbán, JINR Rapid Comm., N3 **89**, 31 (1998).
4. V. Framery *et al.*, *Hydra Topical Manual TQ Title Package*, CERN Program Library (1982).
5. A. Fridman, Forts. Phys. **23**, 243 (1975).
6. B.S. Aladashvili *et al.*, J. Phys. G: Nucl. Phys. **3**, 7 (1977).
7. G. Braun *et al.*, Yad. Fiz. **59**, 2001 (1996).
8. V. Flaminio *et al.*, CERN-HERA 84-01 (1984).
9. A.B. Migdal, JETP **28**, 3 (1955); K.M. Watson, Phys. Rev. **88**, 1163 (1952).
10. A.M. Baldin, Nucl. Phys. A **447**, 203c (1985).
11. V.V. Glagolev *et al.*, JINR Rapid Comm., N3 **89**, 37 (1998).